Science Translational Medicine
AAAS

# Supplementary Materials for

## Blocking $\alpha_4\beta_7$ integrin delays viral rebound in $SHIV_{SF162P3}$-infected macaques treated with anti-HIV broadly neutralizing antibodies

Ines Frank *et al*.

Corresponding author: Elena Martinelli, elena.martinelli@northwestern.edu

*Sci. Transl. Med.* **13**, eabf7201 (2021)
DOI: 10.1126/scitranslmed.abf7201

**The PDF file includes:**



**Other Supplementary Material for this manuscript includes the following:**

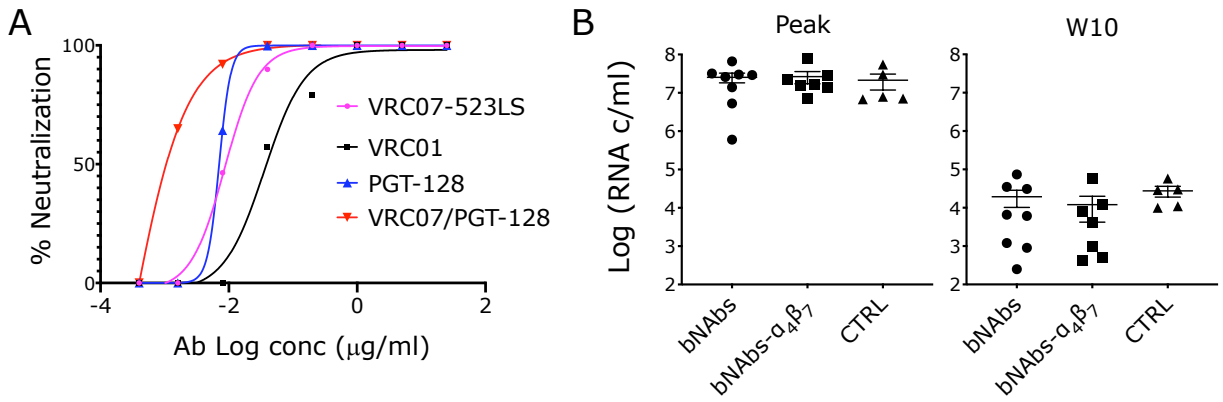


**Supplemental Figure S1. The SHIV-SF126P3 inoculum was sensitive to VRC07-5236LS and PGT128 *in vitro* and the 3 treatment groups had similar peak and pre-treatment plasma viral load.** A) Neutralization of the SHIV-SF162P3 challenge stock by VRC07-523LS, PGT128 and VRC01 WT used as control. Neutralization was measured in macaque PBMC, where 100% virus growth inhibition was achieved at <0.01mg/ml for VRC07-523LS and PGT128. B) The SIV copies/ml of plasma are shown at peak (2 weeks p.i. for IV infected animals and 3 weeks p.i. for IVAG infected animals) and before antibodies infusion at week 10p.i.

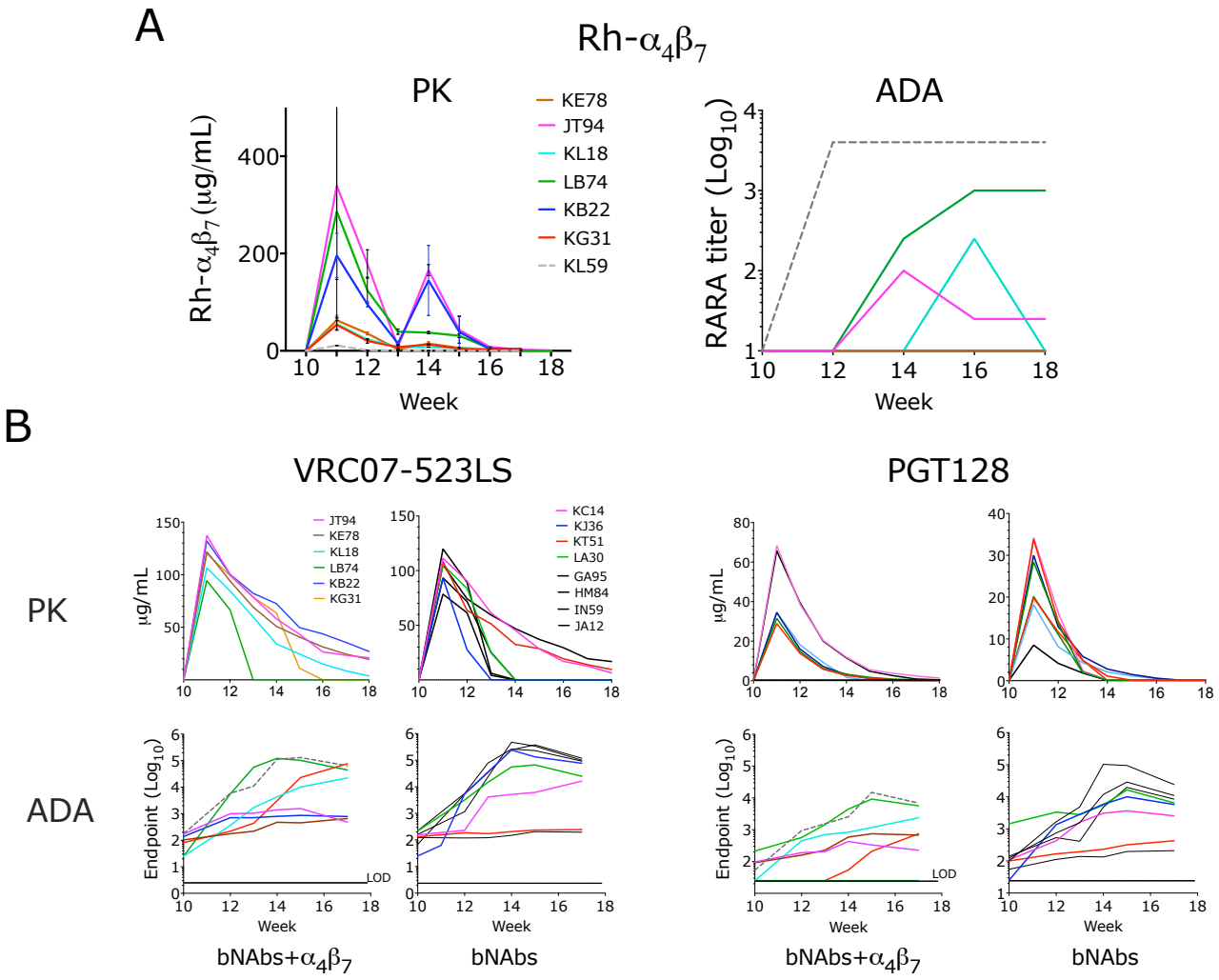


**Supplemental Figure 2. Levels of Rh-α4β7, VRC07-523LS and PGT128 and their respective anti-drug antibodies (ADA).** A-B) The plasma concentrations of Rh-α4β7, bNAbs and ADA are shown for each animal after treatment and for the following 8 weeks. A) Concentrations of Rh-α4β7 (left) and ADA against Rh-α4β7 (right) are shown. The dotted gray line represents the data from the animal (KL59) that was excluded from all subsequent analysis because of the high ADA concentrations. For simplicity, animals infused at week 11/14 with Rh-α4β7 were overlapped to those infused at week 10/13.

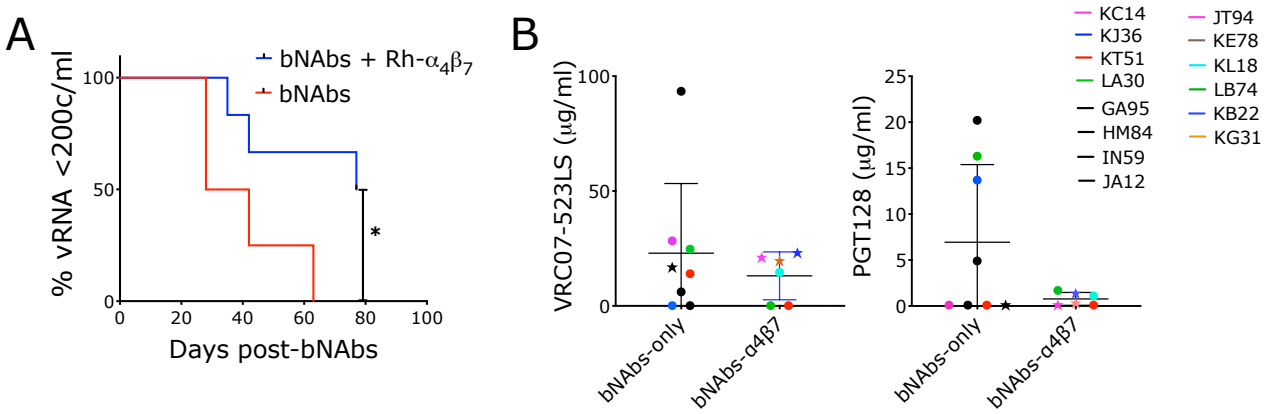


**Supplemental Figure S3. Analysis of time to rebound with only IV infected animals and bNAbs level comparison expanded to non-rebound animals at necropsy. A)** Kaplan-Meier curves generated with time to first detection of >200copies/ml in plasma for IV infected animals in both treatment groups are shown. Curves were compared with the Log-rank test (p=0.039) **B)** Concentrations (mean ± SDs) of VRC07-523LS and PGT128 in plasma before rebound (solid circles) and at necropsy (starts) is shown for both bNAbs-treated group.

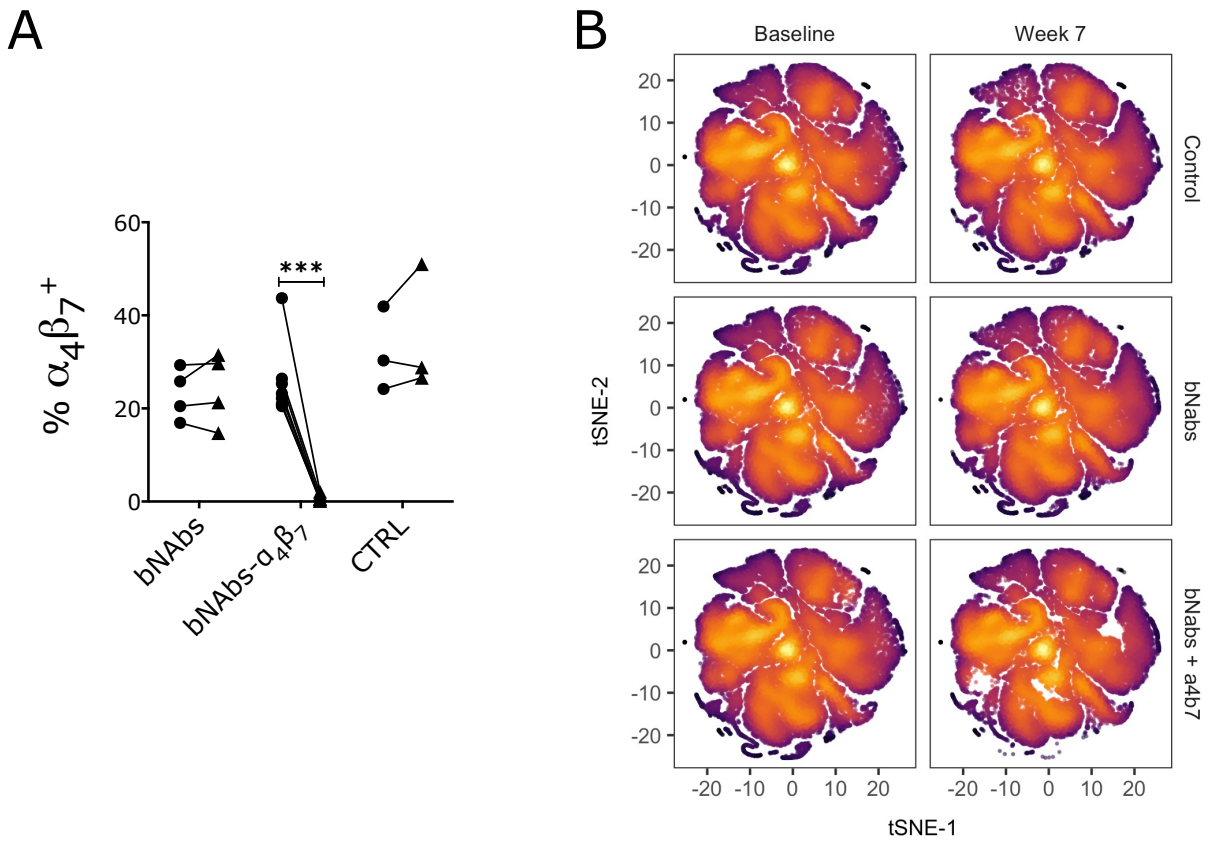


**Supplemental Figure S4. The Rh-$\alpha_4\beta_7$ fully covers the $\alpha_4\beta_7$ receptor expressed by CD4$^+$ T cells. A)** The frequencies of $\alpha_4\beta_7$+ CD4$^+$ T cells within live cells isolated from PBMC at week 10 (W10) and 17 (W17) post-infection are shown. Data were compared by 2-way ANOVA with Sidak multiple comparisons correction. **B)** B) tSNE plots showing kinetic changes in Rh-$\alpha_4\beta_7$-bNabs group at week 17pi. (week 7 post-treatment)

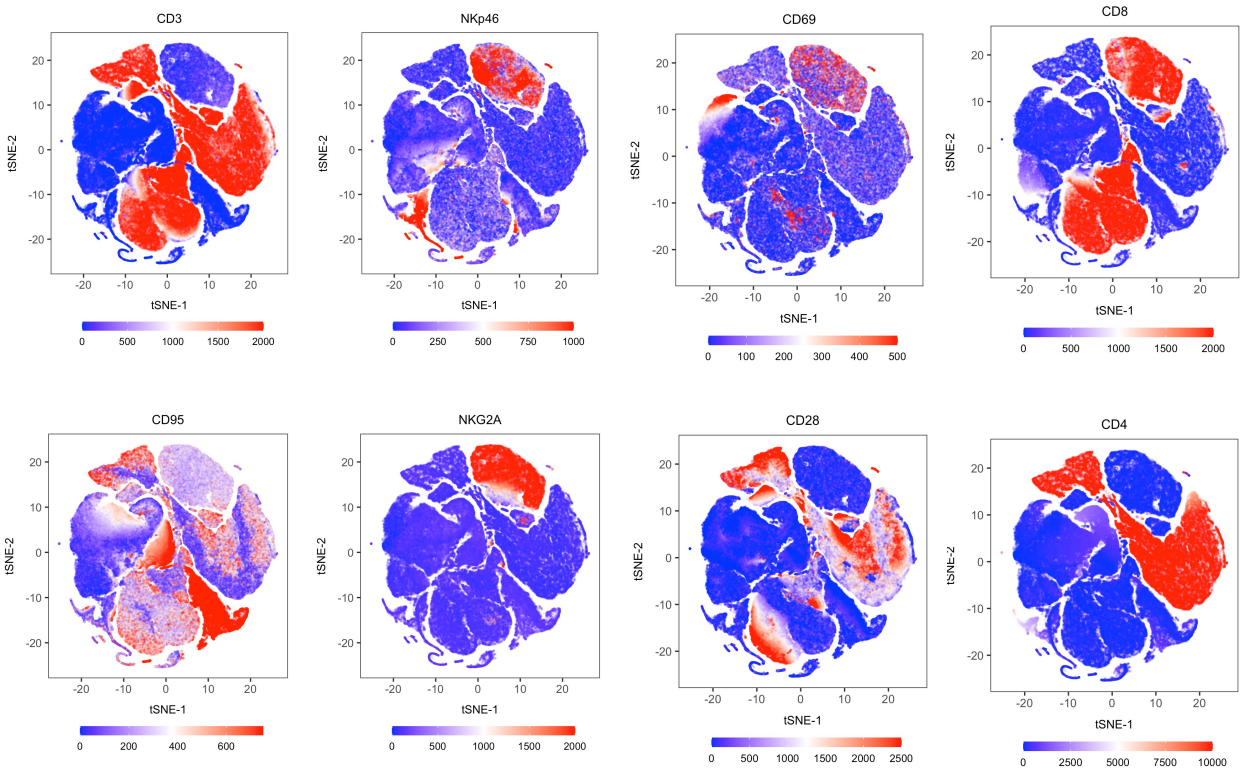


**Supplemental Figure S5. tSNE plots for single marker analysis.** tSNE plots displaying regions of CD3, NKP46, CD69, CD8, CD95, NKG2A, CD28, CD4 expression on live/ singlet cell populations in blood.

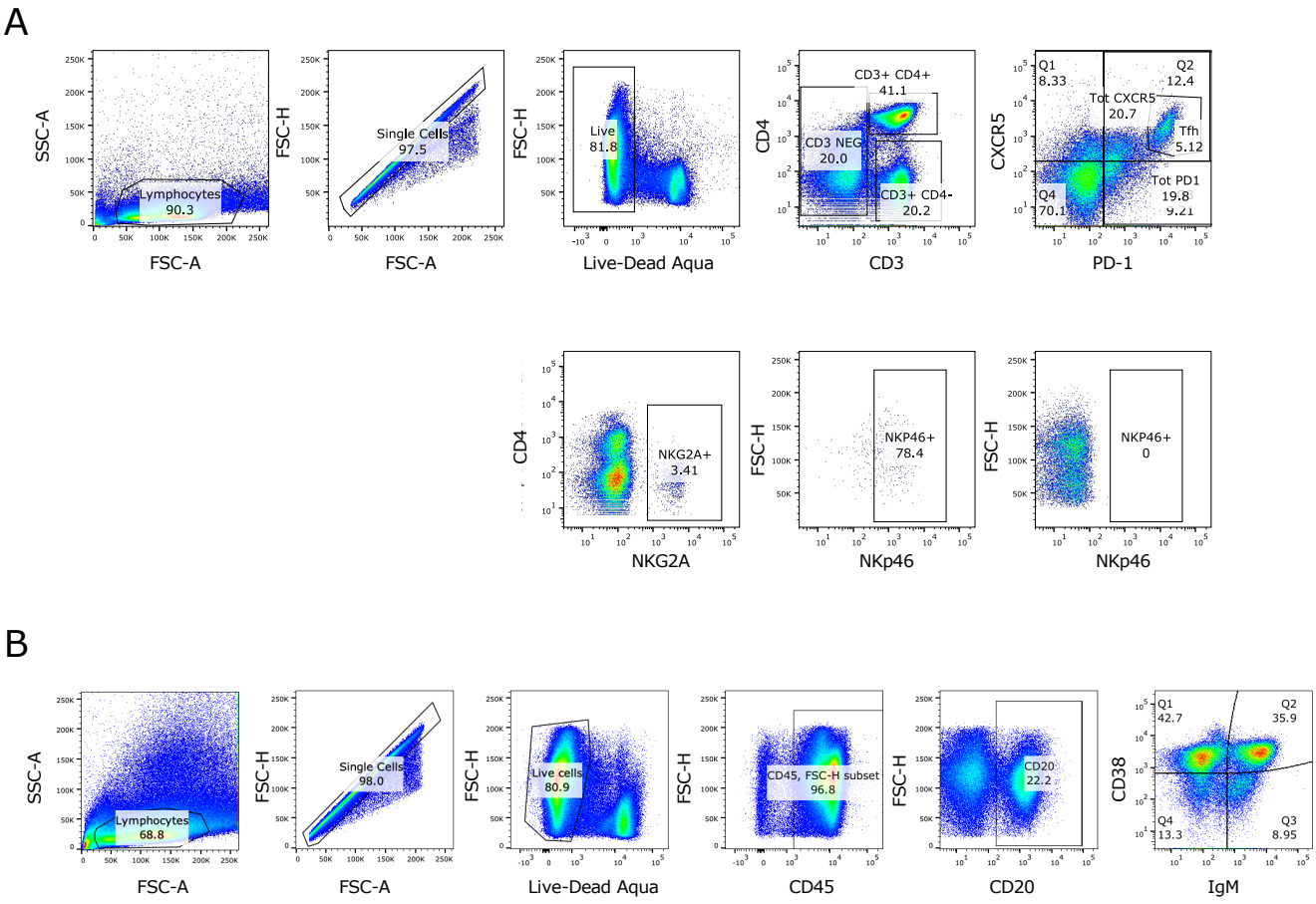


**Supplemental Figure S6. Gating strategy for cell subsets in LNs and gut tissue.** A) The gating strategy for the T/NK panel includes subsets of T cells ($CD4^+$ and $CD4^-$; specifically: Tfh is shown) and NK subsets ($NKG2A^+$ within $CD3^-$). Cells shown were isolated from a lymph node biopsy from KE78. B) The gating strategy for CD38 and IgM is shown for the B cell panel in tissues.

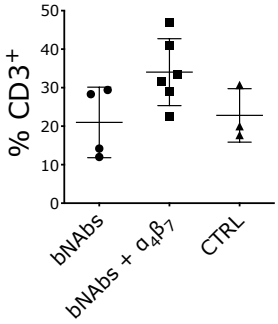


**Supplemental Figure S7. A tendency toward higher frequency of CD3$^+$ T cells was noted in the MLN of Rh-$\alpha_4\beta_7$-bNAbs treated macaques.** Frequency of CD3$^{+\ T}$ cells within live /singlets isolated from MLN are shown. Data were compared with the control by Kruskal-Wallis test and the results of the Dunn's multiple comparisons post-hoc test (*p*-values are >0.05 and are reported in Supplemental Table S4)

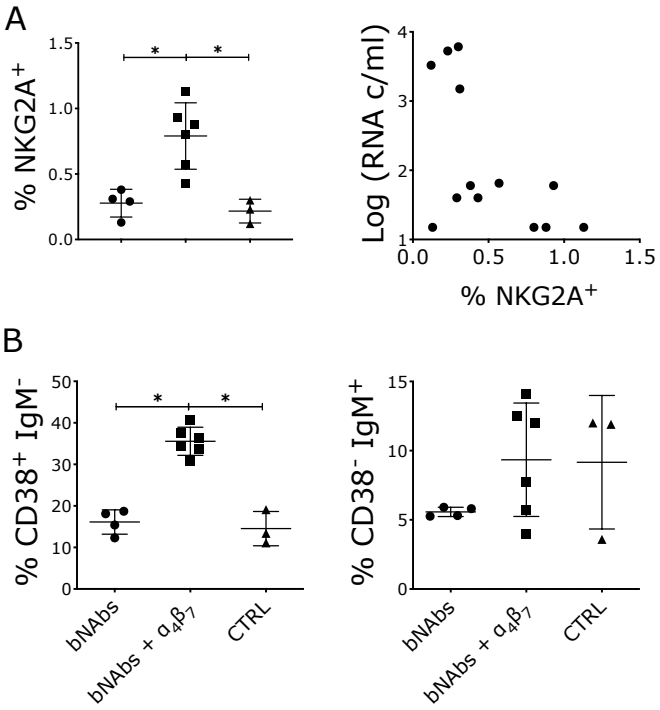


**Supplemental Figure S8. Increased NK cells in MLN and CD38$^+$ IgM$^-$ B cells in the ileum of Rh-$\alpha_4\beta_7$-bNAbs treated macaques.** A) The frequencies of NKG2A$^+$ cells within CD3$^-$ live cells isolated from MLN at necropsy are shown by group and in correlation with pVL at necropsy. B) Frequency of CD38$^+$ IgM$^-$ within CD20$^+$ within CD45$^+$ cells isolated from a small portion of ileum at necropsy are shown. Data from the treatment groups were compared with the control by Kruskal-

Wallis test and the results of the Dunn's multiple comparisons post-hoc test (*p*-value of *α<0.05 and **α <0.01 were considered significant). Bars represent means ± SD.

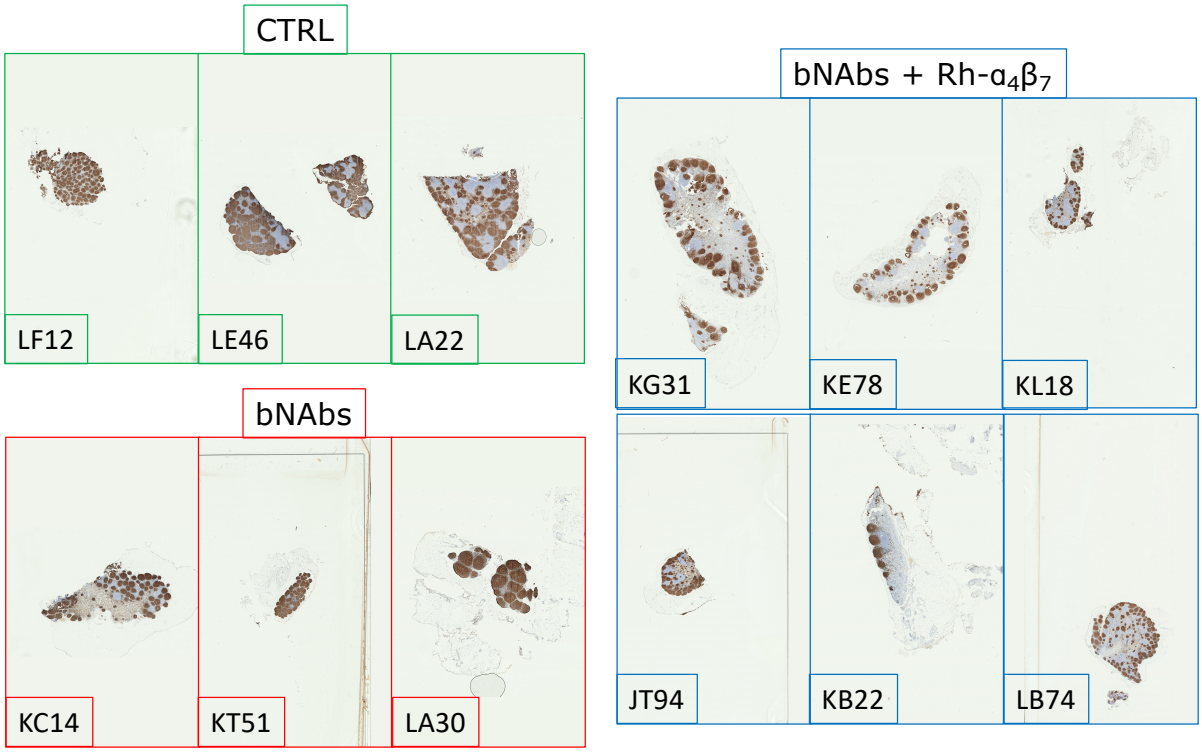


**Supplemental Figure S9. Decreased B-cell follicles in MLN of Rh-α4β7-bNAbs treated macaques.** Full scale histological images of CD20 staining of 1 out of 2 sections of MLN from the 3 treatment groups (KJ37 from the bNAbs only group is shown in main Figure 5A)

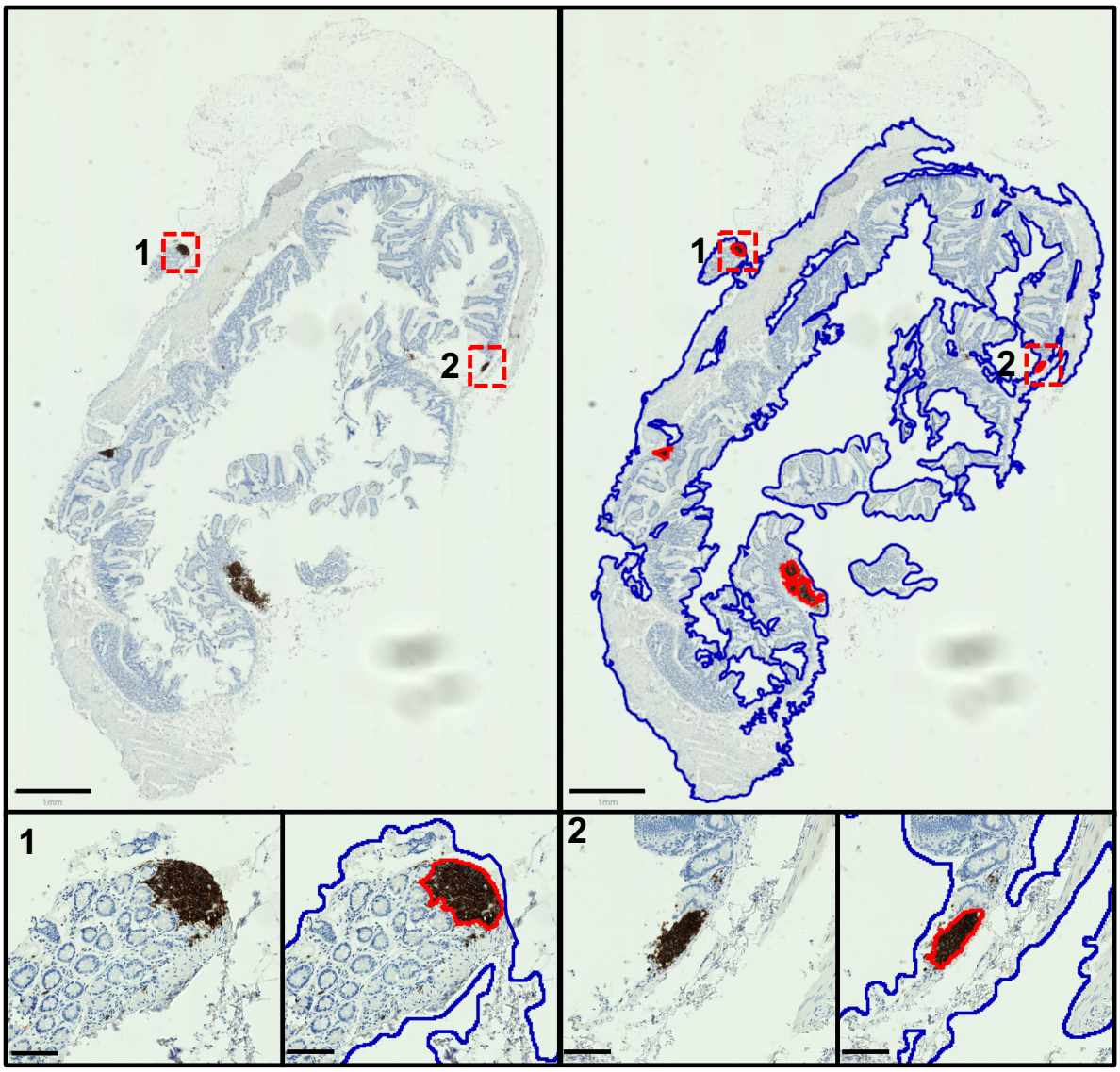


**Supplemental Figure S10 The extent of tissue covered with lymphoid aggregates was measured with QuPath.** The *simple tissue detection* tool was used to create annotation of the tissue regions to be analyzed (tissue boundary in blue). Tissue regions with and without B-cell aggregates (red color) were included for training of artificial neural network (ANN-MLP) classifier using *Pixel Classifier* tool. Full image scale bar is 1mm and insets are 100**µ**m.

**Table S5. List of antibodies used for phenotyping PBMC and tissues**

| Marker | Dye | Clone | Manufacturer |
|---|---|---|---|
| CD3 | AF700 | SP34-2 | BD Biosciences |
| CD4 | BUV395 | L200 | BD Biosciences |
| CD8 | PCP-Cy5.5 | SK1 | BD Biosciences |
| CD95 | V450 | DX2 | BD Biosciences |
| NKG2A | FITC | REA110 | Miltenyi |
| α4β7 | PE | Act-1 | NHP repository |
| CD28 | APC-Vio770 | 1.5E09 | Miltenyi |
| CD38 | APC | OKT10 | NHP repository |
| CD69 | BV605 | FN50 | BD Biosciences |
| CCR7 | BV605 | G043H7 | BioLegend |
| NKp46 | PE-Cy7 | BAB281 | Beckman Coulter |
| CCR6 | PE-Dazzle 594 | G034E3 | BioLegend |
| CD185 | eFluor 450 | MU5UBEE | eBioscience |
| CD279 (PD1) | PerCPeF710 | eBioJ105 (J105) | eBioscience |
| CD159a (NKG2A) | FITC | REA110 | Miltenyi Biotec |
| CD45 | BV605 | D058-1283 | BD Biosciences |
| CD20 | V450 | L27 | BD Biosciences |
| CD27 | PE Vio770 | REA449 | Miltenyi Biotech |
| CD38 | APC | OKT10 | NHP repository |
| CD80 | AF700 | 2D10 | BioLegend |
| CD64 | PE | 10.1 | BD Biosciences |
| HLA-DR | PCP-Cy5.5 | L200 | BD Biosciences |
| IgM | AF488 | G20-127 | BD Biosciences |
| IL-17A | PE | eBio64DEC17 | eBioscience |
| IFN-$_{\gamma}$ | Alexa Fluor 700 | B27 | BD Biosciences |
| TNF-α | FITC | MAb11 | BioLegend |
| IL-2 | BV605 | MQ1-17H12 | BioLegend |